# Density Functional Theory Study of the Mechanism of the Rhodium(I)-Catalyzed Conjugated Diene Assisted Allylic C−H Bond Activation and Addition to Alkenes Using Ene-2-dienes As Substrates

Qian Li and Zhi-Xiang Yu*

Beijing National Laboratory of Molecular Sciences and Key Laboratory of Bioorganic Chemistry and Molecular Engineering of Ministry of Education, College of Chemistry and Molecular Engineering, Peking University, Beijing 100871, China

Ⓢ Supporting Information

ABSTRACT: Recently we reported the first conjugated diene assisted, rhodium-catalyzed allylic C−H bond activation and addition to alkenes to synthesize multifunctional tetrahydropyrroles, tetrahydrofurans, and cyclopentanes from ene-2-diene substrates, with good to excellent diastereoselectivities. Here we report a DFT study of the mechanism of this reaction, aiming to obtain a detailed potential energy surface, to understand factors determining its stereochemistry, and to determine why conjugated diene is very critical for the success of this reaction. DFT calculations unveiled that the catalytic cycle of this reaction involves a sequence of substrate−catalyst complex formation, allylic C−H activation, alkene insertion into the Rh−H bond, and di-π-allyl-assisted $C(sp^3)$−Rh−$C(sp^3)$ reductive elimination, among which the C−H activation and alkene insertion steps are reversible. The main reason for the formation of the cis-divinyl product is that the irreversible reductive elimination transition state from the bis-allylic Rh complex favors a cis 5/5 bicyclic conformation to reduce the ring strain. Moreover, formation of the cis-divinyl product is also assisted by the alkene coordination to the Rh center in the reductive elimination transition state. DFT insights revealed that the conjugated diene, which is very critical for the target reaction, disfavors the double-bond isomerization and facilitates the reductive elimination for the bis-allylic Rh complex, causing the C−H activation and alkene insertion to occur. The computational results showed that the bridgehead double-bond distortion, as suggested by the Bredt's rule, is responsible for not generating the type II [4+2] cycloadducts from ene-2-dienes.
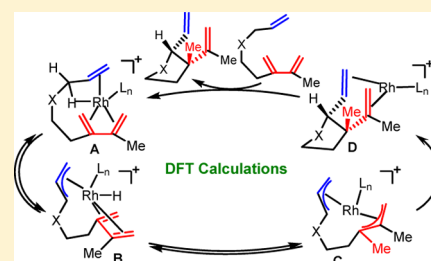
INTRODUCTION

Selective C−H functionalization represents one of the most efficient and straightforward methods to access complex molecules from ubiquitous C−H groups. [1] Among various C−H activation/C−C formation reactions, the additions of C−H bonds across multiple bonds such as alkenes and alkynes are particularly appealing due to their atom- and step-economies.[2] Compared with the additions of aromatic C−H bonds to multiple bonds, the additions of aliphatic C−H bonds to multiple bonds are more challenging due to the inertness of aliphatic C−H bonds and problems related to chemo-, regio-, and stereoselectivities. Although many efforts have been directed to the activation of C−H bonds adjacent to heteroatoms or double bonds,[3] only a limited number of catalytic additions of allylic C−H bonds to alkynes and allenes have been successfully realized.[4−6] In particular, catalytic addition of an allylic C−H bond to alkenes has not been achieved until we serendipitously discovered the first conjugated diene assisted, rhodium-catalyzed allylic C−H bond activation and addition to alkenes, furnishing multifunctional tetrahydropyrroles, tetrahydrofurans, and cyclopentanes, with good to excellent diastereoselectivities between the two newly formed stereogenic centers in the final products (Scheme 1).[7,8] We found this reaction unexpectedly since our original attempt was to develop a Rh-catalyzed formal intramolecular

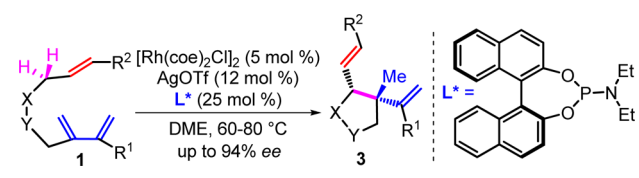**Scheme 1. Conjugated Diene Assisted Allylic C−H Activation and Addition to Alkenes**
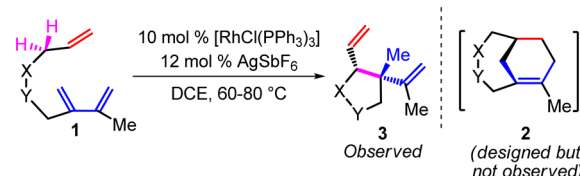
type II Diels−Alder reaction for the synthesis of bridged [4+2] cycloadducts.[9] The allylic C−H activation/addition reactions in Scheme 1 have several advantages. First, the present allylic C−H activation reaction can overcome the regioselectivity challenges, as only the specific allylic C−H bond in the ene part of the substrates can be activated by the Rh catalyst.[10] Second, the reactivity issue on how to realize the formation of an arduous $C(sp^3)$−$C(sp^3)$ bond after the C−H functionalization has also been settled, leading to the generation of quaternary carbon centers in the final products.[11] Third, the diastereoselectivity issue in the final products has also been well

controlled. In addition, an asymmetric version of this reaction has also been developed by us (Scheme 2).[12,13h]

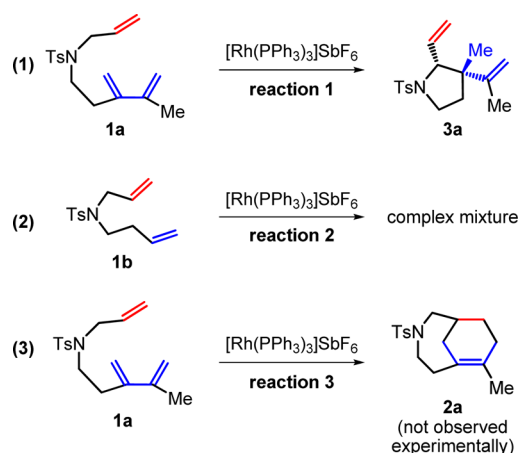**Scheme 2. Asymmetric Allylic C−H Activation and Addition to Alkenes**

The proposed catalytic cycles for the conjugated diene assisted allylic C−H activation/addition reaction and the competing type II [4+2] cycloaddition of ene-2-diene **1a** are shown in Figure 1. The allylic C−H activation/addition reaction is proposed to commence with a ligand exchange reaction between the product−Rh(I) complex **D**, and the substrate **1a**. Through this process, the allylic C−H activation/ addition product **3a** is released and the substrate−Rh(I) complex **A** is generated. The conjugated diene assisted allylic C−H activation then takes place, giving a π-allyl-diene-Rh(III) complex **B**, which is then transformed to a di-π-allyl-Rh(III) complex **C** through alkene insertion of the inner ene part of the conjugated diene into the Rh−H bond. Finally, reductive elimination generates a C(sp³)−C(sp³) bond, affording a product−Rh(I) complex **D** (Figure 1, right). The competitive but disfavored type II [4+2] cycloaddition should also begin with the exchange reaction between cycloadduct **2a**−Rh(I) complex **F** and the substrate **1a**. Through this process, the [4+2] cycloadduct could be released. Then oxidative cyclo-metalation of **A** would take place, giving a π-allyl-Rh(III) complex **E**. Through reductive elimination, this complex would generate a cycloadduct−Rh(I) complex **F**, with which a new catalytic cycle could start again (Figure 1, left).

Discovering new reactions and applying these reactions to impact synthesis are important. Understanding how these reactions occur at the molecular level is of the same importance to advance our knowledge of chemistry and to guide

development of new reactions and catalysts. Therefore, we were interested in applying density functional theory (DFT) calculations to understand how the C−H activation reactions shown in Schemes 1 and 2 occur at the molecular level. Meanwhile, DFT calculations were used to explain the stereochemistry of the target reaction, which gives the cis-divinyl products predominantly. In addition, what is the effect of the indispensible conjugated diene part on the success of the allylic C−H activation/addition reactions? In other words, why can conjugated diene but not a single ene moiety achieve the allylic C−H activation/addition reactions? Moreover, why is our originally designed type II [4+2] cycloaddition totally inhibited for the ene-2-diene substrates? To answer the above questions, three reactions have been investigated using DFT calculations (Scheme 3). The first reaction studied is the C−H

Scheme 3. Three Reactions Studied by DFT Calculations

activation/addition reaction of the ene-2-diene substrate **1a** using triphenylphosphine as the ligand. From the potential energy surface of this reaction, the detailed mechanism of the allylic C−H activation/addition transformation was obtained, and the rate- and stereodetermining steps were disclosed as well. We have also studied reaction **2** to disclose the
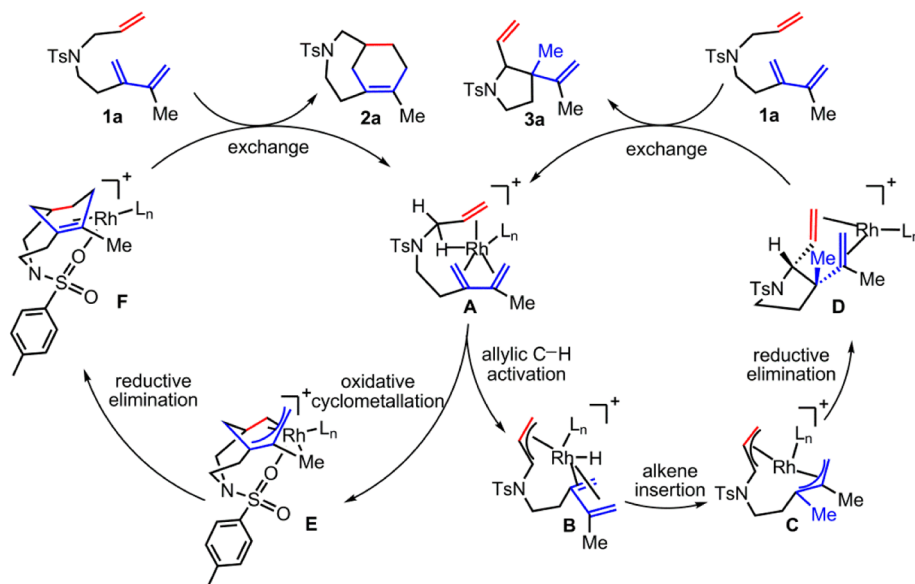

Figure 1. Catalytic cycles for the type II [4+2] cycloaddition and conjugated diene assisted allylic C−H activation/addition reaction.
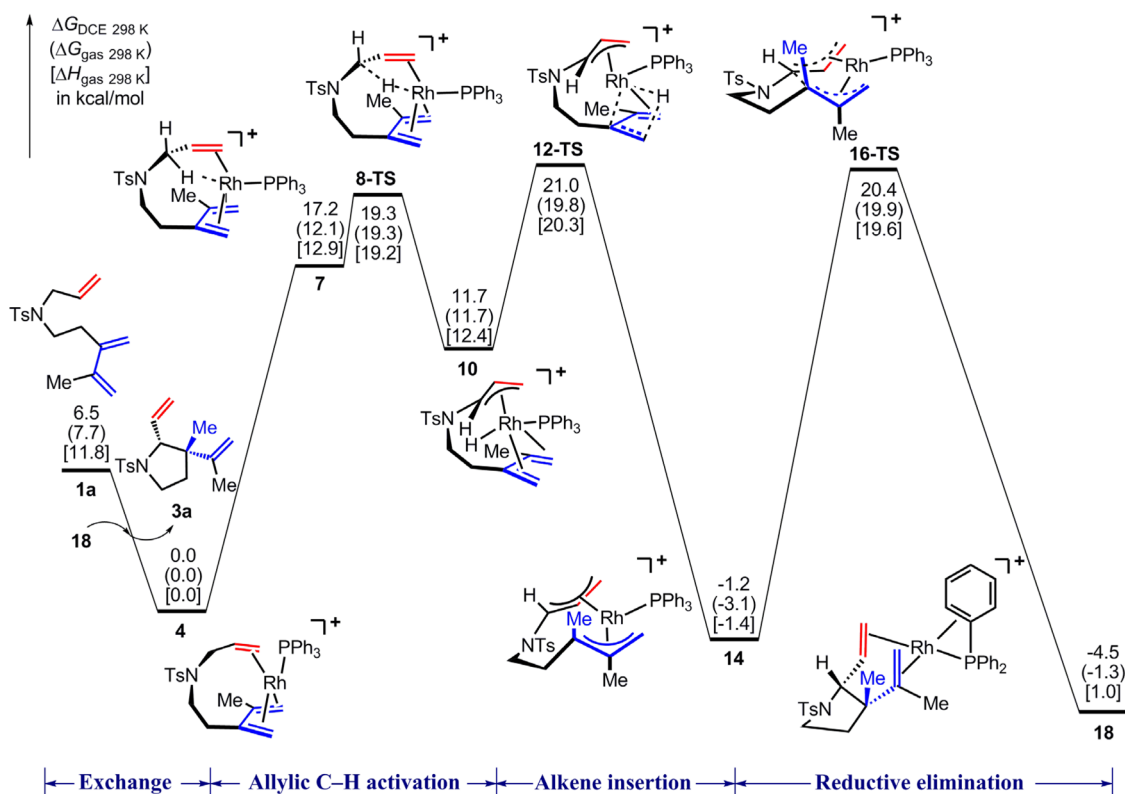
Figure 2. Potential energy surface of the conjugated diene assisted allylic C–H activation and addition to alkene of substrate **1a** (reaction 1).

indispensible role of the conjugated diene moiety on the success of the C−H activation/addition transformation in reaction 1. In addition, DFT calculations to study why the type II [4+2] cycloaddition (reaction 3) of the ene-2-diene **1a** is not feasible compared with reaction 1 will be discussed.

■ COMPUTATIONAL DETAILS

All DFT calculations were performed with the Gaussian 03 software package.[14] Geometry optimization of all the minima and transition states involved was carried out at the B3LYP level of theory[15] at 298 K. The LANL2DZ basis set and pseudopotential[16] were used for the rhodium atom, and the 6-31G(d) basis set[17] was used for other atoms. The keyword "5D" in the Gaussian 03 program was used to specify that five d-type orbitals were used as basis sets in all elements of the calculations. The vibrational frequencies were computed at the same level to check whether each optimized structure is an energy minimum or a transition state and to evaluate its zero-point vibrational energy. Solvent effects were computed on the basis of the gas-phase-optimized structures using the same basis sets.[18] Solvation energies in dichloroethane were evaluated by a self-consistent reaction field using the CPCM model,[19] where the simple united atom topological model (UA0) was used to define the atom radii. In this paper, all discussed energies are Gibbs free energies in dichloroethane ($\Delta G_{DCE\ 298\ K}$) unless specified, where the entropy contributions were estimated by using the gas-phase entropy values. The Gibbs free energies ($\Delta G_{gas\ 298\ K}$) and the enthalpies ($\Delta H_{gas\ 298\ K}$) in the gas phase are also given for reference. Reaction 1 was carried out at 65 °C (338 K), and its Gibbs free energy surface at 65 °C (338 K) is also given in the Supporting Information.[20]

■ RESULTS AND DISCUSSION

1. DFT Investigation of the Energy Profile for the Allylic C−H Activation/Addition Reaction of Ene-2-diene Substrate 1a Using PPh₃ As the Ligand (Reaction 1). The whole potential energy surface of the allylic C−H activation/

addition reaction of ene-2-diene **1a** (reaction 1) is given in Figure 2, and the computed structures are given in Figure 3. The key steps in the catalytic cycle are ligand exchange, allylic C−H activation, alkene insertion into the Rh−H bond, and C(sp³)−C(sp³) bond formation via a reductive elimination process. We will discuss these individual steps below one by one.

Ligand Exchange Step. The allylic C−H activation/addition catalytic cycle starts with the ligand exchange between the product−Rh(I) complex **18**, which is generated in the previous catalytic cycle, and the substrate **1a**. This ligand exchange reaction is exergonic by 6.5 kcal/mol, giving a 16-e Rh(I) complex **4**, in which the ene and conjugated diene moieties in the substrate both coordinate to the Rh(I) center. These two ligands together with a PPh₃ ligand form a square-planar complex around the rhodium center. Complex **4** could be transformed to intermediates **5** and **6** through coordination with another phosphine ligand (Scheme 4). Calculations indicate that complex **5**, with coordination of a diene and two phosphines, is more stable in enthalpy than complex **4** due to the stronger coordination ability of phosphine than alkene. In terms of Gibbs free energy, formation of **5** from **4** and the phosphine ligand is not favored due to its entropy penalty in this process. Formation of the five-coordinated 18-e complex **6** from **4** and PPh₃ is disfavored further, due to entropy reasons as well. In the reaction process, these intermediates could also exist before they are gradually converted to the final product through the elementary steps shown in Figure 2.[21]

Conjugated Diene Assisted Allylic C−H Activation Step. The 16-e complex **4** can adjust its square-planar geometry to a pyramidal-square 18-e complex **7** through formation of an agostic C−H interaction with the Rh center (Figure 2). In complex **7**, the length of the C−H bond is 1.15 Å, while the
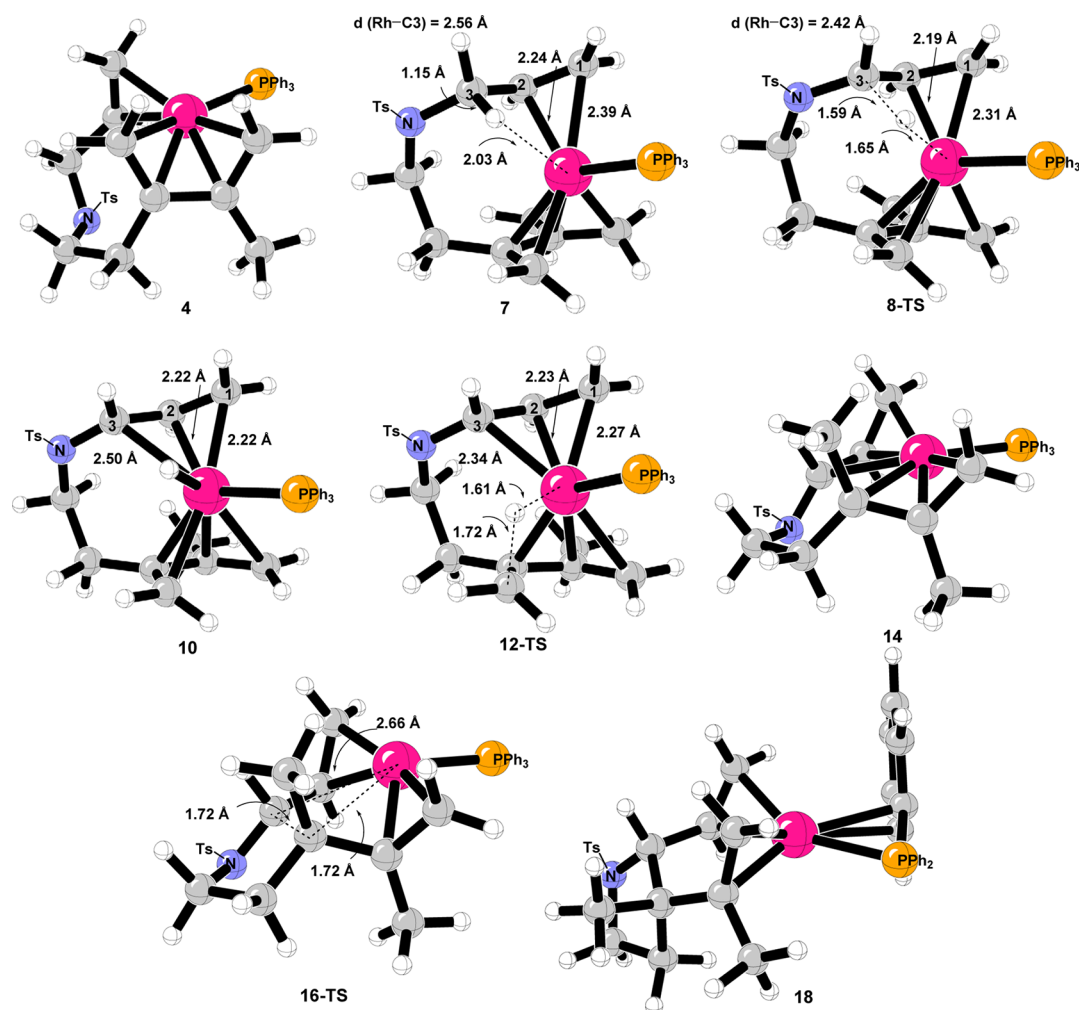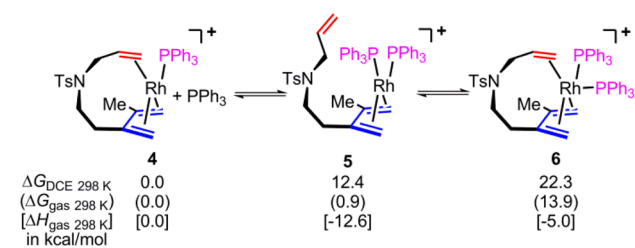
Figure 3. 3D structures of intermediates and transition states in the allylic C−H activation/addition reaction of **1a**. For clarity reasons, in every structure, the PPh₃ and Ts groups are not drawn as 3D models.

Scheme 4. Structures and Energies of Complexes 4, 5, and 6

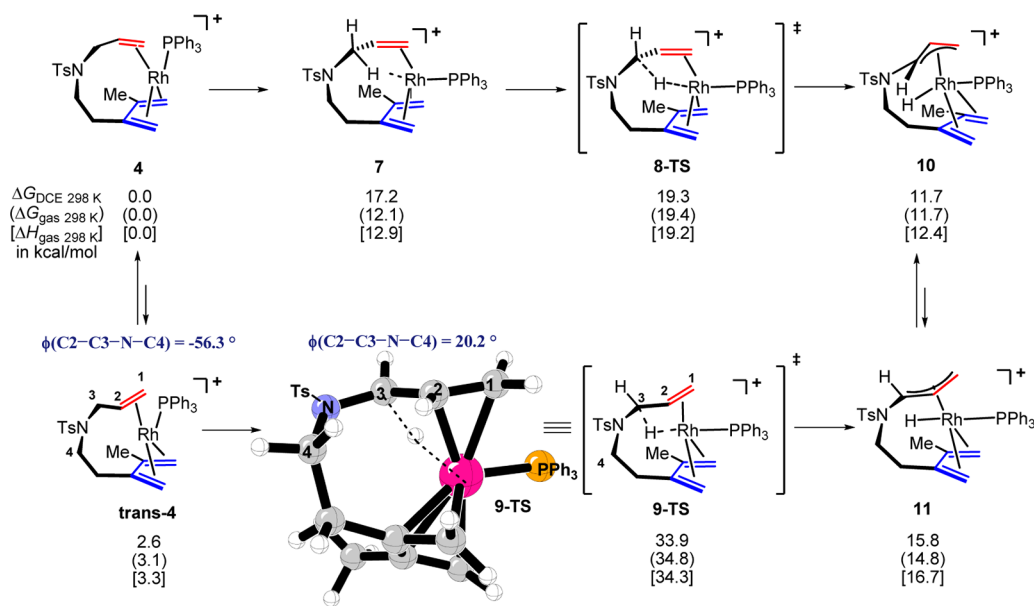|	**4**	**5**	**6**
$\Delta G_{\text{DCE 298 K}}$	0.0	12.4	22.3
$(\Delta G_{\text{gas 298 K}})$	(0.0)	(0.9)	(13.9)
$[\Delta H_{\text{gas 298 K}}]$ in kcal/mol	[0.0]	[-12.6]	[-5.0]

H···Rh bond distance is 2.03 Å.[22] Formation of this agostic complex[23] aims to facilitate the oxidative addition of Rh to the allylic C−H bond via transition state **8-TS**, giving the π-allyl-coordinated Rh complex **10**. The generated Rh−H complex **10** adopts a distorted octahedral configuration, with the PPh₃ ligand and one end of the π-allyl moiety in the axial positions. The C−H activation step has an overall activation free energy of 19.3 kcal/mol (from **4** to **8-TS**). In **7**, **8-TS**, and **10**, the abstracted H atom of the allylic position and the internal alkene part are always in a cis configuration. Such geometric arrangement is to achieve the followed alkene insertion step. Abstraction of the other hydrogen atom of the allylic position in complex **4** (**4** → **trans-4** → **9-TS** → **11**) is not favored due to the fact that **9-TS** is higher in Gibbs free energy than **8-TS**
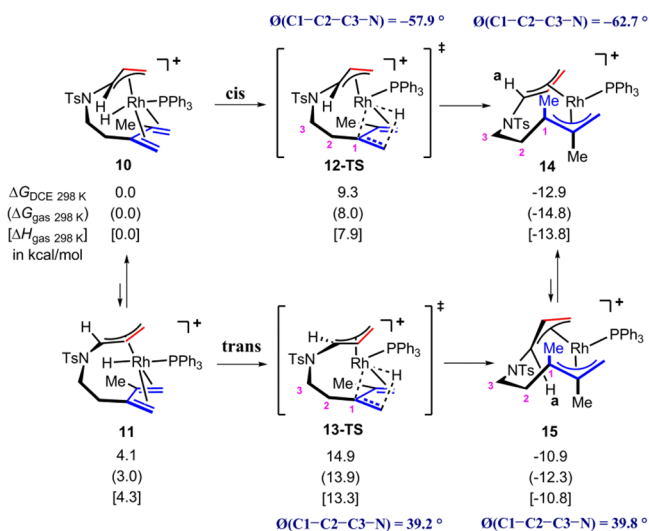
by 14.6 kcal/mol (Scheme 5). This is attributed to the strain energy in **9-TS**, as appreciated from the eclipsed conformation of C2−C3−N−C4 (with a dihedral angle of 20.2°).[24] As suggested by IRC calculations, **9-TS** is not connected by an agostic complex, but by complex **trans-4**, which is higher in energy than complex **4** and has the coordinated alkene adopting a staggered conformation with a dihedral angle of 56.3° for C2−C3−N−C4. Although complex **11** could not be formed through this very energy demanding trans C−H activation transition state **9-TS**, it can still be reached through ligand reorganization process from complex **10** (Scheme 5).

Alkene Insertion into the Rh−H Bond Step. Next, insertion of the inner alkene of the conjugated diene part of **3a** into the Rh−H bond takes place via **12-TS**, giving a cis di-π-allyl-coordinated rhodium complex **14**. This process (**10** → **12-TS** → **14**) requires an activation free energy of 9.3 kcal/mol and is exergonic by 12.9 kcal/mol (Scheme 6). The di-π-allylic Rh complex **14** has the two π-allyl groups adopting a cis configuration with the bridgehead hydrogen, Ha, labeled in Scheme 6 and the newly formed methyl group in the same orientation. There is another possible pathway for the alkene insertion, starting from complex **11** via **13-TS**, to give complex **15**, which has the bridgehead hydrogen, Ha, and the newly formed methyl group in a trans configuration. The insertion step from **11** to **15** is not difficult, with an activation free energy

Scheme 5. DFT-Computed Structures and Energies in the Cis and Trans C−H Activation Processes

	4	**7**	**8-TS**	**10**
$\Delta G_{DCE\ 298\ K}$	0.0	17.2	19.3	11.7
$(\Delta G_{gas\ 298\ K})$	(0.0)	(12.1)	(19.4)	(11.7)
$[\Delta H_{gas\ 298\ K}]$	[0.0]	[12.9]	[19.2]	[12.4]
in kcal/mol				

$\phi(C2-C3-N-C4) = -56.3\ °$ $\phi(C2-C3-N-C4) = 20.2\ °$

	trans-4	**9-TS**	**9-TS**	**11**
	2.6		33.9	15.8
	(3.1)		(34.8)	(14.8)
	[3.3]		[34.3]	[16.7]

Scheme 6. DFT-Computed Structures and Energies in the Cis and Trans Alkene Insertion Processes

Ø(C1−C2−C3−N) = −57.9 °   Ø(C1−C2−C3−N) = −62.7 °

	10	**12-TS**	**14**
$\Delta G_{DCE\ 298\ K}$	0.0	9.3	-12.9
$(\Delta G_{gas\ 298\ K})$	(0.0)	(8.0)	(-14.8)
$[\Delta H_{gas\ 298\ K}]$	[0.0]	[7.9]	[-13.8]
in kcal/mol			

	11	**13-TS**	**15**
	4.1	14.9	-10.9
	(3.0)	(13.9)	(-12.3)
	[4.3]	[13.3]	[-10.8]

Ø(C1−C2−C3−N) = 39.2 °   Ø(C1−C2−C3−N) = 39.8 °

of 10.8 kcal/mol. However, **13-TS** is higher than **12-TS** by 5.6 kcal/mol, suggesting that the alkene insertion from **11** to **15** is not favored kinetically. The high energy of **13-TS** with respect to **12-TS** is still due to the ring strain caused by the eclipsed configuration of the C1−C2−C3−N moieties in both **13-TS** and **15** (these dihedral angles are 39.2° and 39.8°, respectively). Despite this, complex **15** could still be reached from **14** through a ligand reorganization process.

Reductive Elimination Step. The final step of this catalytic cycle is the reductive elimination to form a C(sp³)−C(sp³) bond, giving the product−catalyst complex, with the two stereogenic centers set up simultaneously (Scheme 7).[25] This process, which starts from the cis di-π-allyl intermediate **14** and undergoes reductive elimination via **16-TS**, is exergonic by 3.4 kcal/mol, producing cis divinyl product−catalyst complex **18**. Through a ligand reorganization process, complex **14** can be in equilibrium with the trans 16-e complex **15**, which can also undergo reductive elimination via **17-TS** to give the trans-

product−Rh complex **19**. However, generation of complex **19** and later on the trans-divinyl product is disfavored both kinetically and thermodynamically.

The reason for the preference of generating the cis-divinyl product can be understood by the 5/5 bicyclic ring model (Scheme 8). It has been shown that the 5/5 bicyclic system prefers to adopt a cis conformation for the bridgehead carbon atoms to reduce the ring strain in the two five-membered rings.[26] The formations of **18** and **19** can be viewed as generating two bicyclic 5/5 ring skeletons. Generation of the cis-bicyclic 5/5 ring from **14** to **18** is expected to be favored over generation of the trans 5/5 ring from **15** to **19**.

In addition, the coordination of the divinyl moieties to the Rh center also affects the stereochemistry. For the Rh-(alkene)₂P(PPh₃) complex, the two alkenes favor adopting a parallel configuration.[27] In **16-TS**, the two alkene parts still have a parallel configuration ($\Phi(C1-C2-C3-C4) = -12.1°$), while in **17-TS**, the two alkene parts have a crossover configuration ($\Phi(C1-C2-C3-C4) = -68.1°$), making the latter transition state further disfavored in terms of alkene coordination. Complexes **18** and **19** also reflect this difference, with the former being more stable than the latter by 11.3 kcal/mol. Since **16-TS** is favored over **17-TS** kinetically by 1.4 kcal/mol in solution, the final product is dominated by generating the cis-divinyl products. This is consistent with the experimental observation.[28]

In summary, the whole potential energy surface of the catalytic cycle for the conjugated diene assisted allylic C−H activation/addition to alkenes, which is shown in Figure 2, indicates that the conversion from substrate **1a** to complex **4** via ligand exchange is exergonic by 6.5 kcal/mol. The allylic C−H activation step (via **8-TS**) is relatively facile and requires an activation free energy of 19.3 kcal/mol. The alkene insertion step (via **12-TS**) and the reductive elimination step (via **16-TS**) are the competitive rate-determining steps, which require activation free energies of 21.0 and 21.6 kcal/mol, respectively. As the interconversion between **14** and **15** is facile, the diastereoselectivity of this reaction should be determined by the final reductive elimination step, which is irreversible and gives the thermodynamically more stable cis divinyl product−catalyst

Scheme 7. Relative Energies of the Competing Reductive Elimination Steps
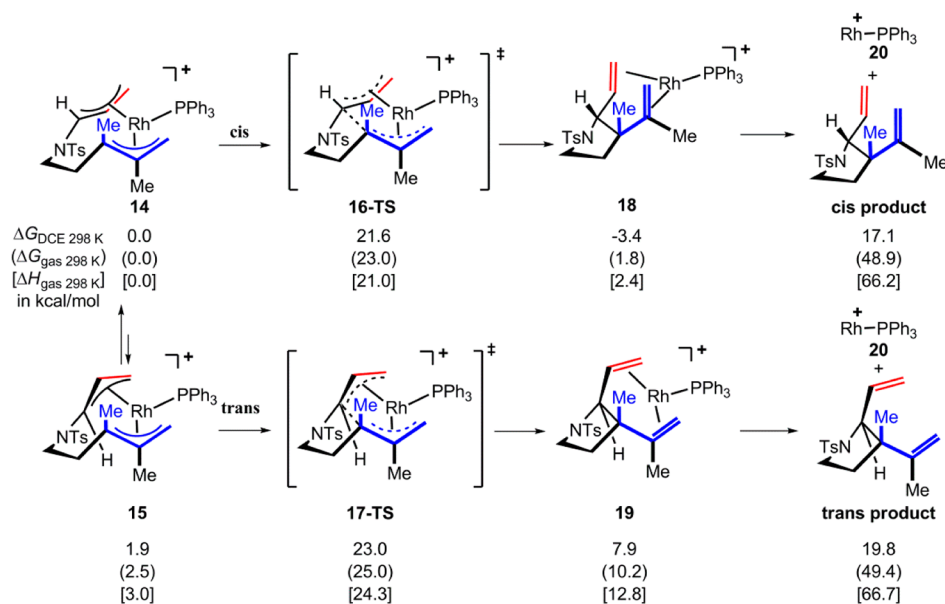
**Scheme 8. 5/5 Bicyclic Model for Rationalization of the Cis Selectivity**
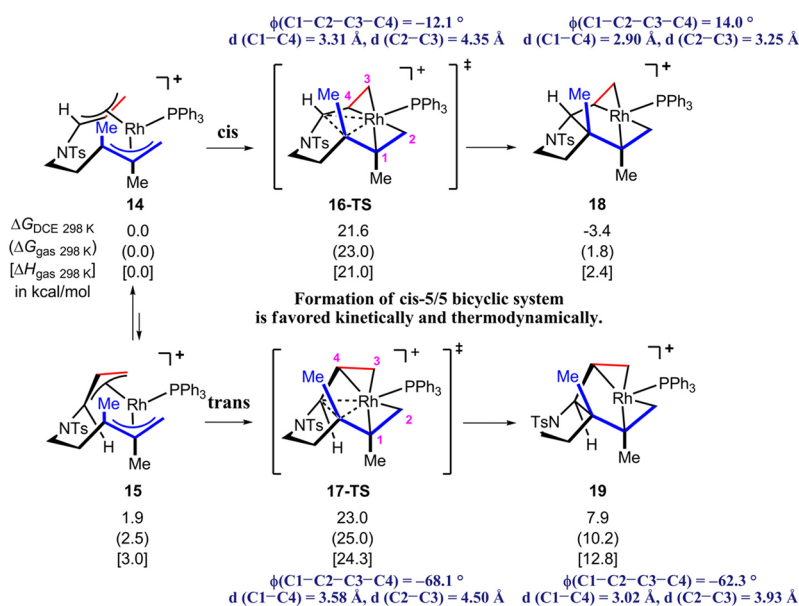
complex **18**. The overall activation free energy of this allylic C−H activation/addition reaction is 21.6 kcal/mol, which is in good agreement with the experimental fact that this allylic C−H activation/addition reaction readily occurs at 65 °C and delivers the cis-divinyl-substituted product **3a** predominantly.

Before concluding this part, we point out here that there is another possible pathway giving the final product (Scheme 9). This pathway starts from alkene insertion into the Rh−C bond[29] via **21-TS**, instead of the Rh−H bond via **12-TS**, to give complex **22**, which then undergoes reductive elimination to give the final product. We found this step is very difficult, requiring an activation free energy of 41.1 kcal/mol from the Rh−H intermediate **10**. Therefore, this pathway can be ruled out for further consideration. This is in good agreement with our previous isotopic labeling experiments, which support the alkene insertion into the Rh−H bond but not the Rh−C bond. The main reason for the difficult alkene insertion into the Rh−

C bond is that such a process would break the stronger η^3 coordination of the allylic group in transition state **21-TS**, in which the C1 and C2 atoms are not coordinated to the Rh center.

2. Why Is the Conjugated Diene Moiety in the Ene-2-diene Substrate Indispensable for the Success of the Allylic C−H Activation/Addition Reactions? In order to determine why the conjugated diene moiety is important for the target reactions of ene-2-diene substrates, we synthesized bis-ene substrate **1b**, which does not have a conjugated diene moiety, to test whether the same reaction sequence happening in ene-2-diene **1a** can also take place with **1b**. When **1b** was subjected to the allylic C−H activation/addition reaction conditions ([Rh(PPh₃)₃Cl], AgSbF₆, 70 °C, DCE as solvent), only a complex mixture was observed, without giving any desired five-membered adduct **3b**, as judged by the NMR spectra of the crude reaction mixtures (Scheme 10). We

Scheme 9. Structures and Energies in the Alkene Insertion into the Rh−C Bond
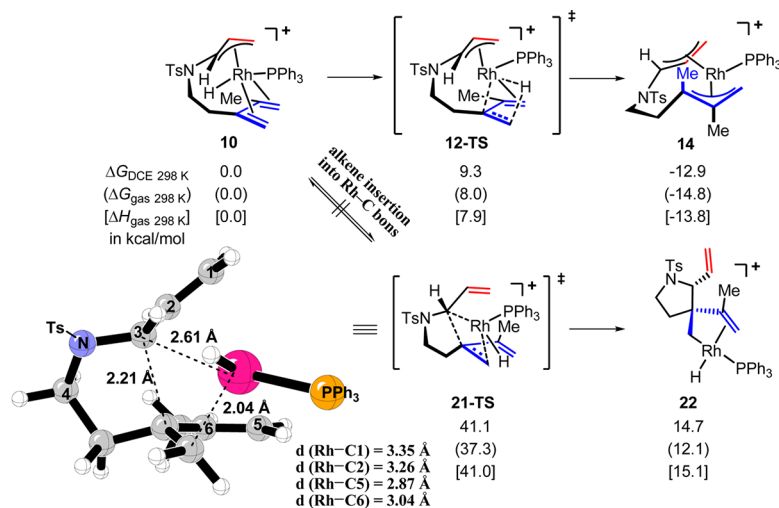
Scheme 10. Reaction of Bis-ene Substrate 1b
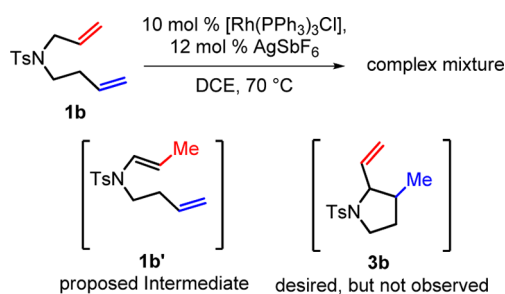
proposed that this reaction first generated enamine intermediate **1b′** through Rh-catalyzed double-bond isomerization, which was not stable and immediately decomposed to a complex mixture of unidentified products.[30]

DFT calculations were performed to determine why **1b** could not generate **3b** (Figure 4). Herein, we used the ene-2-diene **1a** instead of bis-ene **1b** to do the calculations. In the calculations, the outer ene unit of the conjugated diene moiety in **1a** was treated as a substituent and did not take part in the coordination to the Rh center.[31] Without the complexation of a conjugated diene moiety, the most stable substrate−Rh complex is the nitrogen-coordinated, phosphine-stabilized, square-planar substrate−Rh complex **23**. DFT calculations
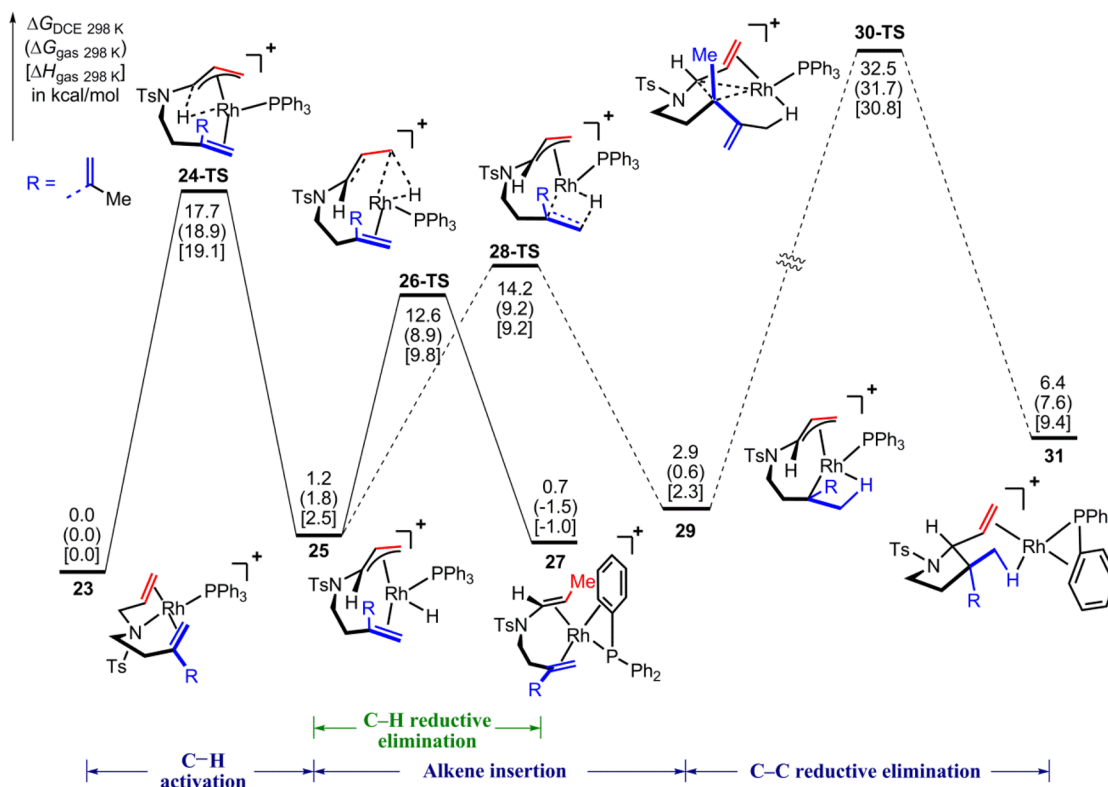
Figure 4. Potential energy surface of the bis-ene substrate **1b** (reaction 2, here the R group can be regarded as a simple substituent in **1a**).

Scheme 11. Effect of Conjugated Diene on Tuning the Chemoselectivity of Ene-2-diene Substrates
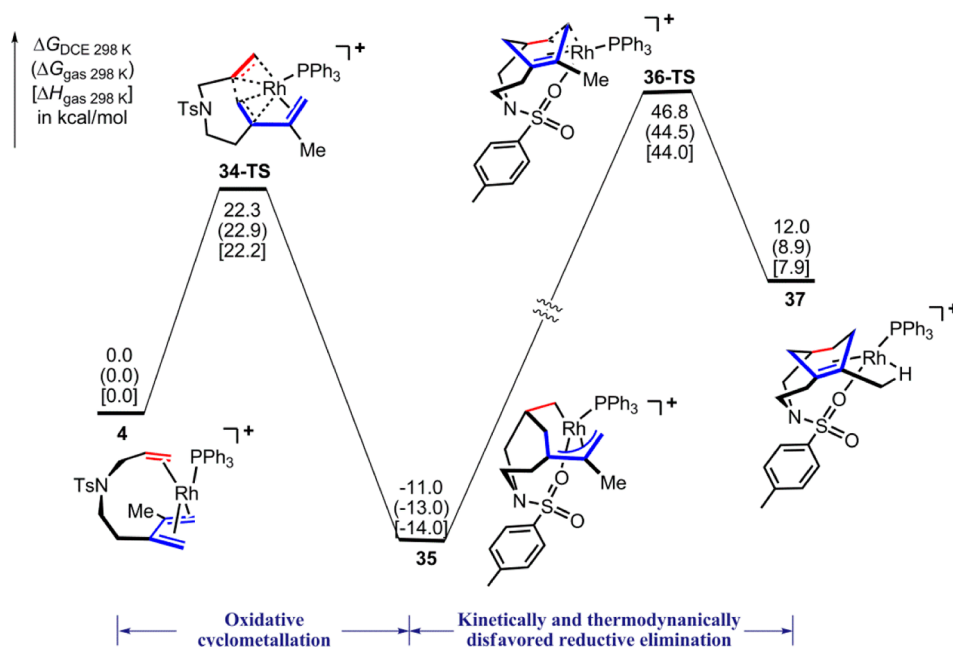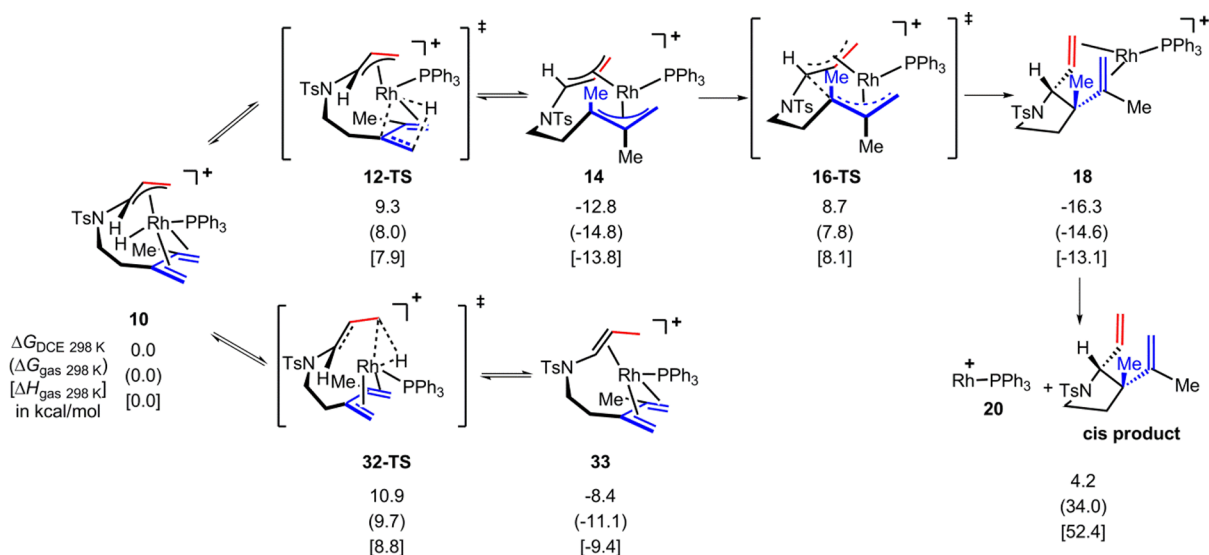

Figure 5. Potential energy surface of type II [4+2] cycloaddition of ene-2-diene substrate **1a** (reaction 3).

suggest that the generation of an alkene isomerization product is also the result of allylic C−H activation. C−H activation via **24-TS** is an energetically neutral process with an activation free energy of 17.7 kcal/mol, generating Rh−H complex **25**. After the allylic C−H activation step, there are two competitive pathways for further transformations. One is a direct reductive elimination via **26-TS** to give isomerization product−Rh complex **27**. Alternatively, similar to reaction **1**, the alkene moiety can insert into the Rh−H bond via **28-TS**, giving intermediate **29**, which then undergoes reductive elimination via **30-TS** to generate complex **31**.

Our DFT calculations found that generation of **27** is favored over the generation of **31**, because **30-TS** is 19.9 kcal/mol higher than **26-TS**. This suggests that reaction of **1b** could give product **1b′** through a C−H bond formation via a reductive elimination process. **1b′** is an enamine, which is not stable and

could undergo unexpected reactions to give a mixture of unidentified products.

The most important reason for not generating **3b** is that the reductive elimination via **30-TS** requires an overall activation free energy of 32.5 kcal/mol. The other reason is the disfavored alkene insertion into the Rh−H bond (via transition state **28-TS**) with respect to the reductive elimination process via transition state **26-TS** (the energy difference is 1.6 kcal/mol). This suggests that, in the reaction system, **25**, **27**, and **29** could be in equilibrium, but they will reach **30-TS** with difficulty. Consequently, other unexpected side reactions from **25**, **27**, and **29** could occur and thus give a mixture of unidentified products. We attribute the higher activation energy for **30-TS** to the lack of stabilizing coordination group around the 16-e Rh center, which is stabilized by an agostic interaction instead of a more favorable alkene moiety. Moreover, this disadvantaged reductive elimination step can be further appreciated by the
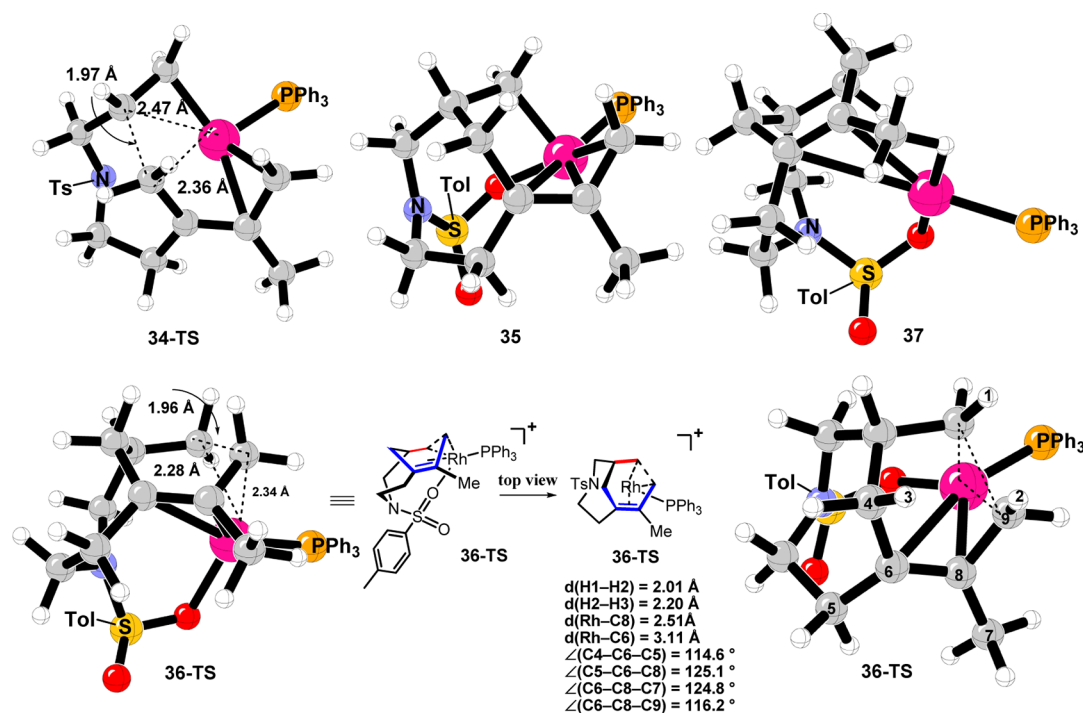
Figure 6. 3D structures of intermediates and transition states in the type II [4+2] cycloaddition. For clarity reasons, in every structure, the PPh$_3$, Ts, and Tol groups are not drawn as 3D models.

endothermicity of the reductive elimination process from **29** to **31**.[32]

The above discussion suggests that without the conjugated diene moiety, double-bond isomerization is easier. However, when the conjugated diene is present, the competitive double-bond isomerization process via **32-TS**, which is a reversible process, is disfavored compared with the alkene insertion into the Rh–H bond via **12-TS** (Scheme 11).

Calculations found that the isomerization of intermediate **10** to **33** via the C–H bond reductive elimination transition state **32-TS** requires an activation free energy of 10.9 kcal/mol, 1.6 kcal/mol higher than the alkene insertion into the Rh–H bond process via **12-TS**. Therefore, complex **10** prefers to give complex **14**, which then undergoes an irreversible reductive elimination reaction to furnish the divinyl product. The energy difference between **32-TS** and **12-TS** is only 1.6 kcal/mol, suggesting that intermediate **33** could be generated in the reaction process. But the reaction from **10** to **18** is irreversible. Therefore, intermediate **10** will finally give the divinyl product via **12-TS** and **16-TS**.

From the above analysis, we can conclude that the presence of the conjugated diene affects the reaction pathway in two ways. One is to disfavor the double-bond isomerization process. The other is to facilitate the reductive elimination from the bis-π-allylic Rh complex **14**.

3. Why Is the Type II [4+2] Pathway Not Favored? In this part, we computed the energy surface of the originally expected but not realized type II [4+2] reaction pathway of **1a** to understand why this pathway is not favored (Figure 5). Calculations indicate that the oxidative cyclometalation between the ene moiety and the internal ene part of the conjugated diene in the ene-2-diene substrate from complex **4** is not difficult, requiring an activation free energy of 22.3 kcal/mol. This step gives the thermodynamically stable oxygen-coordinated intermediate **35**. However, the reductive elimi-

nation reaction from **35** to form the C–C bond is energetically forbidden because this step requires an activation free energy of 57.8 kcal/mol. Since the C–H activation pathway to generate the Rh–H species **10** is much easier, with an activation free energy of 19.3 kcal/mol (Figure 2), the type II [4+2] pathway is impossible when the Rh catalyst is applied.

Analysis of the reductive elimination transition structure **36-TS** reveals that two factors are responsible for the high activation energy of this step. One factor is due to the formation of a bridgehead double bond, which leads to a remarkable distortion energy according to Bredt's rule.[33] This severe distortion can be understood from the geometry of the forming C6=C8 double bond. As shown in Figure 6, the angles around the forming C=C double bond are twisted away from 120°, with angles C4–C6–C5, C5–C6–C8, C6–C8–C7, and C6–C8–C9 being 114.6°, 125.1°, 124.8°, and 116.2°, respectively. The distortion of the double bond in the forming six-membered ring causes serious strain, thus making this transition structure rather energetically demanding. Second, steric repulsions in this very congested reductive elimination transition state, **36-TS**, cannot be ignored. As shown in Figure 6, the distances between the labeled hydrogen atoms in the forming six-membered ring, H1–H2 and H2–H3, are only 2.01 and 2.20 Å, which are shorter than the sum of their van der Waals radii (2.40 Å).[34] In addition, the reductive elimination in this pathway is endergonic by 12.2 kcal/mol, making this pathway thermodynamically disfavored.

■ CONCLUSION

The mechanism of the Rh(I)-catalyzed allylic C–H activation/addition reactions of ene-2-diene substrates has been investigated by DFT calculations. The present mechanistic study reveals the detailed processes of the catalytic cycles, the potential energy profile, and the structures of intermediates and transition states.

Insights obtained in the present DFT study include the following: (a) The catalytic cycle of the allylic C−H activation/addition reactions includes the substrate−catalyst complex formation, allylic C−H activation, alkene insertion into the Rh−H bond, and di-π-allyl-assisted reductive elimination to form the C(sp^3)−C(sp^3) bond. (b) Formation of the cis-divinyl product is due to the fact that the reductive elimination transition state from the bis-allylic Rh complex prefers to adopt a cis 5/5 conformation to reduce the ring strain. Formation of the cis-divinyl product is also assisted by alkene coordination to the Rh center in the reductive elimination transition state. (c) The conjugated diene is very important to disfavor the double-bond isomerization and facilitate the reductive elimination for the bis-allylic Rh complex. (d) In addition, the computational results show that the bridgehead double-bond distortion, suggested by Bredt's rule, is responsible for not generating the type II [4+2] cycloadducts from ene-2-dienes.

The present DFT study provides an understanding of the rhodium-catalyzed C−H activation reactions of conjugated-diene-containing substrates, and we hope these insights could serve as a mechanistic guide to inspire future discovery of new conjugated diene assisted reactions. Further studies of the substituent effects and how ligands affect the kinetics and stereochemistry of the present C−H activation/addition to alkenes reactions are ongoing and will be reported in due course.

■ ASSOCIATED CONTENT

Ⓢ Supporting Information

Computational details, discussions of computational methods, and computed energies and Cartesian coordinates of all stationary points are available free of charge via the Internet at http://pubs.acs.org.

■ AUTHOR INFORMATION

Corresponding Author
*E-mail: yuzx@pku.edu.cn.
Notes
The authors declare no competing financial interest.

■ ACKNOWLEDGMENTS

■ REFERENCES

(1) (a) Kakiuchi, F.; Chatani, N. *Adv. Synth. Catal.* **2003**, *345*, 1077. (b) Dick, A. R.; Sanford, M. S. *Tetrahedron* **2006**, *62*, 2439. (c) Godula, K.; Sames, D. *Science* **2006**, *312*, 67. (d) Bergman, R. G. *Nature* **2007**, *446*, 391. (e) Chen, M. S.; White, M. C. *Science* **2007**, *318*, 783. (f) Chen, X.; Engle, K. M.; Wang, D. H.; Yu, J.-Q. *Angew. Chem., Int. Ed.* **2009**, *48*, 5094. (g) Ackermann, L. *Chem. Rev.* **2011**, *111*, 1315. (h) Wencel-Delord, J.; Droege, T.; Liu, F. *Chem. Soc. Rev.* **2011**, *40*, 4740. (i) Baudoin, O. *Chem. Soc. Rev.* **2011**, *40*, 4902. (j) Lyons, T. W.; Sanford, M. S. *Chem. Rev.* **2010**, *110*, 1147. (k) Shi, W.; Liu, C.; Lei, A. *Chem. Soc. Rev.* **2011**, 2761. (l) Hartwig, J. F. *Acc. Chem. Res.* **2012**, *45*, 864. (m) Davies., H. M. L.; Du Bois, J.; Yu, J.-Q. *Chem. Soc. Rev.* **2011**, *40*, 1855. (n) Engle, K. M.; Mei, T.-S.; Wasa, M.; Yu, J.-Q. *Acc. Chem. Res.* **2012**, *45*, 788. (o) Wencel-Delord, J.; Dröge, T.; Liu, F.; Glorius, F. *Chem. Soc. Rev.* **2011**, *40*, 4740. (p) Hashiguchi, B. G.; Bischof, S. M.; Konnick, M. M.; Periana, R. A. *Acc. Chem. Res.* **2012**, *45*, 885.
(2) (a) Jia, C.; Kitamura, T.; Fujiwara, Y. *Acc. Chem. Res.* **2001**, *34*, 633. (b) Ritleng, V.; Sirlin, C.; Pfeffer, M. *Chem. Rev.* **2002**, *102*, 1731.

(c) Kakiuchi, F.; Murai, S. *Acc. Chem. Res.* **2002**, *35*, 826. (d) Colby, D. A.; Bergman., R. G.; Ellman, J. A. *Chem. Rev.* **2010**, *110*, 624.
(3) (a) Campos, K. R. *Chem. Soc. Rev.* **2007**, *36*, 1069. (b) Li, Z.; Bohle, D. S.; Li, C.-J. *Proc. Natl. Acad. Sci. U. S. A.* **2006**, *103*, 8928. (c) Li, C.-J. *Acc. Chem. Res.* **2009**, *42*, 335. (d) Chen, M. S.; White, M. C. *J. Am. Chem. Soc.* **2004**, *126*, 1346. (e) Young, A. J.; White, M. C. *J. Am. Chem. Soc.* **2008**, *130*, 14090. (f) Liu, G.; Yin, G.; Wu, L. *Angew. Chem., Int. Ed.* **2008**, *47*, 4733. (g) Liu, W.; Liu, J.; Ogawa, D.; Nishihara, Y.; Guo, X.; Li, Z. *Org. Lett.* **2011**, *13*, 6277.
(4) (a) Trost, B. M.; Toste, F. D. *J. Am. Chem. Soc.* **1999**, *121*, 9728. (b) Lei, A.; He, M.; Zhang, X. *J. Am. Chem. Soc.* **2002**, *124*, 8198. (c) Ajamian, A.; Gleason, J. L. *Org. Lett.* **2003**, *5*, 2409. (d) Brummond, K. M.; Chen, H.; Mitasev, B.; Casarez, A. D. *Org. Lett.* **2004**, *6*, 2161. (e) Li, W.; Yuan, W.; Shi, M.; Hernandez, E.; Li, G. *Org. Lett.* **2010**, *12*, 64. For an oxidative coupling: (f) Franzén, J.; Bäckvall, J. E. *J. Am. Chem. Soc.* **2003**, *125*, 6056.
(5) For Alder-ene cycloisomerization reactions: (a) Sturla, S. J.; Kabalaeui, N. M.; Buchwald, S. L. *J. Am. Chem. Soc.* **1999**, *121*, 1976. (b) Trost, B. M.; Lautens, M.; Chan, C.; Jebaratnam, D. J.; Muller, T. *J. Am. Chem. Soc.* **1991**, *113*, 636. (c) Trost, B. M.; Toste, F. D. *J. Am. Chem. Soc.* **2000**, *122*, 714. (d) Cao, P.; Wang, B.; Zhang, X. *J. Am. Chem. Soc.* **2000**, *122*, 6490. (e) Fürstner, A.; Majima, K.; Martín, R.; Krause, H.; Kattnig, E.; Goddard, R.; Lehmann, C. W. *J. Am. Chem. Soc.* **2008**, *130*, 1992.
(6) For the transition metal catalyzed addition of C−H bonds adjacent to a heteroatom to alkenes and alkynes, see: (a) Chatani, N.; Asaumi, T.; Yorimitsu, S.; Ikeda, T.; Kakiuchi, F.; Murai, S. *J. Am. Chem. Soc.* **2001**, *123*, 10935. (b) Sakaguchi, S.; Kubo, T.; Ishii, Y. *Angew. Chem., Int. Ed.* **2001**, *40*, 2534. (c) Shi, L.; Tu, Y.-Q.; Wang, M.; Zhang, F.-M.; Fan, C.-A.; Zhao, Y.-M.; Xia, W.-J. *J. Am. Chem. Soc.* **2005**, *127*, 10836. (d) Herzon, S. B.; Hartwig, J. F. *J. Am. Chem. Soc.* **2008**, *130*, 14940. (e) McQuaid, K. M.; Sames, D. *J. Am. Chem. Soc.* **2009**, *131*, 402. (f) Zhang, S.-Y.; Tu, Y.-Q.; Fan, C.-A.; Zhang, F.-M.; Shi, L. *Angew. Chem., Int. Ed.* **2009**, *48*, 8761. To alkynes: (g) Shikanai, D.; Murase, H.; Hata, T.; Urabe, H. *J. Am. Chem. Soc.* **2009**, *131*, 3166. (h) Tsuchikama, K.; Kasagawa, M.; Endo, K.; Shibata, T. *Org. Lett.* **2009**, *11*, 1821. (i) Gao, K.; Yoshikai, N. *Angew. Chem., Int. Ed.* **2011**, *50*, 6888. (j) Lee, P.-S.; Fujita, T.; Yoshikai, N. *J. Am. Chem. Soc.* **2011**, *133*, 17283. (k) Ryu, J.; Cho, S. H.; Chang, S. *Angew. Chem., Int. Ed.* **2012**, *51*, 3677. (l) Minami, Y.; Shiraishi, Y.; Yamada, K.; Hiyama., T. *J. Am. Chem. Soc.* **2012**, *134*, 6124. (m) Nakao, Y.; Morita, E.; Idei, H.; Hiyama, T. *J. Am. Chem. Soc.* **2011**, *133*, 3264.
(7) Li, Q.; Yu, Z.-X. *J. Am. Chem. Soc.* **2010**, *132*, 4542.
(8) Nakamura, I.; Yamamoto, Y. *Chem. Rev.* **2004**, *104*, 2127.
(9) Transition metal catalyzed intramolecular type I D−A reactions: (a) Wender, P. A.; Jenkins, T. E. *J. Am. Chem. Soc.* **1989**, *111*, 6432. (b) Jolly, R. S.; Luedtke, G.; Sheehan, D; Livinghouse, T. *J. Am. Chem. Soc.* **1990**, *112*, 4965. (c) Wender, P. A.; Jenkins, T. E.; Suzuki, S. *J. Am. Chem. Soc.* **1995**, *117*, 1843. (d) Wender, P. A.; Smith, T. E. *J. Org. Chem.* **1996**, *61*, 824. (e) Gilbertson, S. R.; Hoge, G. S. *Tetrahedron Lett.* **1998**, *39*, 2075. (f) Kumar, K.; Jolly, R. S. *Tetrahedron Lett.* **1998**, *39*, 3047. (g) Paik, S. J.; Son, S. U.; Chung, Y. K. *Org. Lett.* **1999**, *1*, 2045. (h) Wang, B.; Cao, P.; Zhang, X. *Tetrahedron Lett.* **2000**, *41*, 8041. (i) Motoda, D.; Kinoshita, H.; Shinokubo, H.; Oshima, K. *Angew. Chem., Int. Ed.* **2004**, *43*, 1860. (j) Yoo, W. J.; Allen, A.; Villeneuve, K.; Tam, W. *Org. Lett.* **2005**, *7*, 5853. (k) Lee, S. I.; Park, S. Y.; Park, J. H.; Jung, I. G.; Choi, S. Y.; Chung, Y. K. *J. Org. Chem.* **2006**, *71*, 91. (l) Saito, A.; Ono, T.; Takahashi, A.; Taguchi, T.; Hanzawa, Y. *Tetrahedron Lett.* **2006**, *47*, 891. (m) Aikawa, K.; Akutagawa, S; Mikami, K. *J. Am. Chem. Soc.* **2006**, *128*, 12648. (n) Arai, S.; Koike, Y.; Hada, H.; Nishida, A. *J. Am. Chem. Soc.* **2010**, *132*, 4522. For a review of type II D−A reactions, see: (o) Bear, B. R.; Sparks, S. M.; Shea, K. J. *Angew. Chem., Int. Ed.* **2001**, *40*, 820.
(10) Trost, B. M.; Crawley, M. L. *Chem. Rev.* **2003**, *103*, 2921.
(11) (a) Netherton, M. R.; Fu, G. C. *Adv. Synth. Catal.* **2004**, *346*, 1525. (b) Frisch, A. C; Beller, M. *Angew. Chem., Int. Ed.* **2005**, *44*, 674. (c) Rudolph, A.; Lautens, M. *Angew. Chem., Int. Ed.* **2009**, *48*, 2656.
(12) For an excellent review of stereoselective C−H bond activation, see: Giri, R.; Shi, B.-F.; Engle, K. M.; Maugel, N.; Yu, J.-Q. *Chem. Soc.*

Rev. **2009**, *38*, 3242. For reviews on enantioselective C−H activation by means of carbene and nitrene insertions, see: (b) Davies, H. M. L.; Manning, J. R. *Nature* **2008**, *451*, 417. (c) Muller, P.; Fruit, C. *Chem. Rev.* **2003**, *103*, 2905. (d) Doyle, M. P.; Duffy, R.; Ratnikov, M.; Zhou, L. *Chem. Rev.* **2010**, *110*, 704.

(13) For recent work on the enantioselective C−H activation: (a) Shi, B.-F.; Zhang, Y.-H.; Lam, J. K.; Wang, D.-H.; Yu, J.-Q. *J. Am. Chem. Soc.* **2010**, *132*, 460. (b) Wasa, M.; Engle, K. M.; Lin, D. W.; Yoo, E. J.; Yu, J.-Q. *J. Am. Chem. Soc.* **2011**, *133*, 19598. (c) Saget, T.; Lemouzy, S. J.; Cramer, N. *Angew. Chem., Int. Ed.* **2012**, *51*, 2238. (d) Reznichenko, A.; Emge, T. J.; Audörsch, S.; Klauber, E. G.; Hultzch, K. C.; Schmidt, B. *Organometallics* **2011**, *30*, 921. (e) Nakanishi, M.; Katayev, D.; Besnard, C.; Kündig, P. E. *Angew. Chem., Int. Ed.* **2011**, *50*, 7438. (f) Yamaguchi, K.; Yamaguchi, J.; Studer, A.; Itami, K. *Chem. Sci.* **2012**, *3*, 2165. (g) Katayev, D.; Nakanishi, M.; Bürgi, T.; Kündig, P. E. *Chem. Sci.* **2012**, *3*, 1422. (h) Li, Q.; Yu, Z.-X. *Angew. Chem., Int. Ed.* **2011**, *50*, 2144. (i) Pan, S.; Endo, K.; Shibata, T. *Org. Lett.* **2011**, *13*, 4692.

(14) Frisch, M. J.; et al. *Gaussian 03*, revision C.02; Gaussian, Inc.: Wallingford, CT, 2004.

(15) (a) Becke, A. D. *J. Chem. Phys.* **1993**, *98*, 5648. (b) Lee, C.; Yang, W.; Parr, R. G. *Phys. Rev. B* **1988**, *37*, 785.

(16) Wadt, W. R.; Hay, P. J. *J. Chem. Phys.* **1985**, *82*, 284.

(17) Hehre, W. J.; Radom, L.; Schleyer, P. v. R.; Pople, J. A. *Ab Initio Molecular Orbital Theory*; Wiley: New York, 1986.

(18) The basis sets we used have been successfully applied to study structures and reaction mechanisms for other rhodium-catalyzed reactions: (a) Yu, Z.-X.; Wender, P. A.; Houk, K. N. *J. Am. Chem. Soc.* **2004**, *126*, 9154. (b) Yu, Z.-X.; Cheong, P. H.-Y.; Liu, P.; Legault, C. Y.; Wender, P. A.; Houk, K. N. *J. Am. Chem. Soc.* **2008**, *130*, 2378. (c) Liu, P.; Cheong, P. H.-Y.; Yu, Z.-X.; Wender, P. A.; Houk, K. N. *Angew. Chem., Int. Ed.* **2008**, *47*, 3939. (d) Liu, P.; Sirois, L. E.; Cheong, P. H.-Y.; Yu, Z.-X.; Hartung, I. V.; Rieck, H.; Wender, P. A.; Houk, K. N. *J. Am. Chem. Soc.* **2010**, *132*, 10127. (e) Nakamura, E.; Yoshikai, N.; Yamanaka, M. *J. Am. Chem. Soc.* **2002**, *124*, 7181. (f) Baik, M.-H.; Baum, E. W.; Burland, M. C.; Evans, P. A. *J. Am. Chem. Soc.* **2005**, *127*, 1602. (g) Montero-Campillo, M. M.; Rodriguez-Otero, J.; Cabaleiro-Lago, E. M. *Tetrahedron* **2008**, *64*, 6215. (h) Wang, H.; Sawyer, J. R.; Evans, P. A.; Baik, M.-H. *Angew. Chem., Int. Ed.* **2008**, *47*, 342. (i) Montero-Campillo, M. M.; Cabaleiro-Lago, E. M.; Rodriguez-Otero, J. *J. Phys. Chem. A* **2008**, *112*, 9068. (j) Liang, Y.; Zhou, H.; Yu, Z.-X. *J. Am. Chem. Soc.* **2009**, *131*, 17783. (k) Hansen, J.; Autschbach, J.; Davies, H. M. L. *J. Org. Chem.* **2009**, *74*, 6555. (l) Jiao, L.; Lin, M.; Yu, Z.-X. *J. Am. Chem. Soc.* **2011**, *133*, 447.

(19) (a) Barone, V.; Cossi, M. *J. Phys. Chem. A* **1998**, *102*, 1995. (b) Cossi, M.; Rega, N.; Scalmani, G.; Barone, V. *J. Comput. Chem.* **2003**, *24*, 669. (c) Takano, Y.; Houk, K. N. *J. Chem. Theory Comput.* **2005**, *1*, 70.

(20) The calculated Gibbs free energies in the gas phase and in DCE at the reaction temperatures (338 K) can be transformed from the calculated free energies in the gas phase and in DCE at 298 K, provided that the entropy in these reactions remains the same at different temperatures. We find that these data have about 0.1 to 0.2 kcal/mol differences from the data reported at 298 K. The potential energy surface of reaction 1 at 338 K is given in the Supporting Information.

(21) We have located another 16-e oxygen-coordinated monophosphine-stabilized complex, **4′**, but this complex is 8.5 kcal/mol higher in Gibbs free energy than complex **4**.
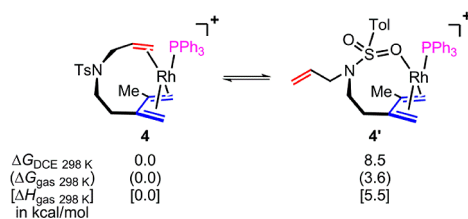
(22) Brookhart, M.; Green, M. L. H.; Parkin, G. *Proc. Natl. Acad. Sci.* **2007**, *104*, 6908.

(23) We have performed the atoms in molecules (AIM) calculations of complex **7**, showing that there is a bond critical point between Rh and the activated allylic hydrogen. The electron density value of this critical point is 0.0444. The eigenvalues are −0.0379, −0.0153, and 0.2259. The corresponding Laplacian value is 0.1727. For more details, please see the Supporting Information.

(24) For selected recent examples, see: (a) Janardanan, D.; Sunoj, R. B. *J. Org. Chem.* **2008**, *73*, 8163. (b) Um, J. M.; Houk, K. N.; Phillips, A. J. *Org. Lett.* **2008**, *10*, 3769. (c) Schoenebeck, F.; Ess, D. H.; Jones, G. O.; Houk, K. N. *J. Am. Chem. Soc.* **2009**, *131*, 8121. (d) Wang, H.; Michalak, K.; Michalak, M.; Jiménez-Osés, G.; Wicha, J.; Houk, K. N. *J. Org. Chem.* **2010**, *75*, 762. (e) Patil, M. P.; Sharma, A. K.; Sunoj, R. B. *J. Org. Chem.* **2010**, *75*, 7310. (f) Shinisha, C. B.; Sunoj, R. B. *J. Am. Chem. Soc.* **2010**, *132*, 12319. (g) Wang, T.; Liang, Y.; Yu, Z.-X. *J. Am. Chem. Soc.* **2011**, *133*, 9343.

(25) For DFT calculations of the transition metal catalyzed allyl−allyl coupling, see: (a) Mendez, M.; Cuerva, J. M.; Gomez-Bengoa, E.; Cardenas, D. J.; Echavarren, A. M. *Chem.—Eur. J.* **2002**, *8*, 3620. (b) Pérez-Rodríguez, M.; Braga, A. A. C.; de Lera, A. R.; Maseras, F.; Álvarez, R.; Espinet, P. *Organometallics* **2010**, *29*, 4983. For examples of allyl−allyl coupling containing heteroatoms, see: (c) Keith, J. A.; Behenna, D. C.; Mohr, J. T.; Ma, S.; Marinescu, S. C.; Oxgaard, J.; Stoltz, B. M.; Goddard, W. A., III. *J. Am. Chem. Soc.* **2007**, *129*, 11876. (d) Chen, J.-P.; Peng, Q.; Lei, B.-L.; Hou, X.-L.; Wu, Y.-D. *J. Am. Chem. Soc.* **2011**, *133*, 14180. (e) Hansen, J. H.; Gregg, T. M.; Ovalles, S. R.; Lian, Y.; Autschbach, J.; Davies, H. M. L. *J. Am. Chem. Soc.* **2011**, *133*, 5076. (f) Ariafard, A.; Lin, Z. *J. Am. Chem. Soc.* **2006**, *128*, 13010.

(26) Gordon, H. L.; Freeman, S.; Hudlicky, T. *Synlett* **2005**, 2911.

(27) Defieber, C.; Grützmacher, H.; Carreira, E. M. *Angew. Chem., Int. Ed.* **2008**, *47*, 4482 , and references therein.

(28) Substituents can affect this stereochemistry, as demonstrated by one substrate giving a final product with dr = 5/1 (see ref 7).

(29) Kakiuchi, F.; Sekine, S.; Tanaka, Y.; Kamatani, A.; Sonoda, M.; Chatani, N.; Murai, S. *Bull. Chem. Soc. Jpn.* **1995**, *68*, 62.

(30) Tan, K. L.; Bergman, R. G.; Ellman, J. A. *J. Am. Chem. Soc.* **2001**, *123*, 2685.

(31) We also calculated the potential energy surface of reaction 2 using bis-ene substrate **1b**, which can be viewed as a model of ene-2-diene **1a** when the outer ene unit is treated as a substituent but not as a ligand. Similar conclusions can be reached to those shown in Figure 4. Details can be seen in the Supporting Information.

(32) In **30-TS**, an agostic C−H coordination to the Rh center exists, but this coordination is not efficient compared to alkene coordination in **16-TS**. It is possible that this reductive elimination would be easier if another PPh$_3$ ligand coordinates to the Rh atom in the reductive elimination transition state. However, in **30-TS**, such a vacant site for coordination by another PPh$_3$ ligand is not available.

(33) (a) Bredt, J. *Justus Liebig's Ann. Chem.* **1924**, *437*, 1. (b) Shea, K. *Tetrahedron* **1980**, *36*, 1683.

(34) Bondi, A. *J. Phys. Chem.* **1964**, *68*, 441.

$\Delta G_{\text{DCE 298 K}}$ ... **4**: 0.0, **4'**: 8.5
$(\Delta G_{\text{gas 298 K}})$ ... (0.0), (3.6)
$[\Delta H_{\text{gas 298 K}}]$ ... [0.0], [5.5]
in kcal/mol